

A Stellar Spectral Flux Library: 1150–25000 Å

A. J. PICKLES

Institute for Astronomy, University of Hawaii, Hilo, HI 96720; pickles@ifa.hawaii.edu

Received 1997 November 10; accepted 1998 March 26

ABSTRACT. A stellar spectral flux library of wide spectral coverage and an example of its application are presented. The new library consists of 131 flux-calibrated spectra, encompassing all normal spectral types and luminosity classes at solar abundance, and metal-weak and metal-rich F–K dwarf and G–K giant components. Each library spectrum was formed by combining data from several sources overlapping in wavelength coverage. The SIMBAD database, measured colors, and line strengths were used to check that each input component has closely similar stellar type. The library has complete spectral coverage from 1150 to 10620 Å for all components and to 25000 Å for about half of them, mainly later types of solar abundance. Missing spectral coverage in the infrared currently consists of a smooth energy distribution formed from standard colors for the relevant types. The library is designed to permit inclusion of additional digital spectra, particularly of non-solar abundance stars in the infrared, as they become available. The library spectra are each given as F_λ versus λ , from 1150 to 25000 Å in steps of 5 Å. A program to combine the library spectra in the ratios appropriate to a selected isochrone is described and an example of a spectral component signature of a composite population of solar age and metallicity is illustrated. The library spectra and associated tables are available as text files by remote electronic access.

1. INTRODUCTION

There are several published stellar libraries, covering the ultraviolet, optical, and infrared spectral ranges. They were obtained with different instrumentation, at different resolutions and spectral sampling and for different purposes, including stellar population synthesis and comparison with theoretical spectral flux calculations. Various groups have successfully used these libraries to suit their programs, either individually or in combinations, as reviewed most recently by Leitherer et al. (1996).

The existing libraries combine considerable utility for specific applications with occasional annoying problems for general use including, sometimes, limited coverage of wavelength, spectral type, or abundance range, poor or doubtful flux calibration or atmospheric feature removal, and the necessity to combine spectra from diverse data sets. The spectral classification of some stars has been refined over the years, which leads to slight inconsistencies in libraries that group spectra by stellar type.

Theoretical stellar spectra are often preferred for spectral modeling because of their uniformity and generally more extensive coverage of stellar type, luminosity class, chemical abundance, and wavelength range. They may be biased in color and line strength, however; there are many minor contributors to stellar opacity and the emergent spectrum, which usually cannot all be included for the full spectral range because of computational constraints. There are also some systematic effects that are attributable to resolvable differences between the-

oretical and observed stellar libraries and to color-temperature (and color-color) calibrations, as reviewed by Charlot, Worthey, & Bressan (1996).

For population synthesis in particular, it is sometimes preferable to model the light from a composite stellar population in terms of observable spectra. The utility of observed spectra for this and for checking theoretical flux calibrations depends on extending their coverage of type, luminosity class, abundance, and wavelength, all of which can clearly be improved.

The objective here is to provide a flux library of observed spectra representing normal stellar types that is as complete and uniform as presently possible, together with a simple and open mechanism for highlighting deficiencies and extending and improving the database as new observations become available. This was done by selecting what are thought to be the best observed spectra in each wavelength interval, grouping them by spectral type, luminosity class, and abundance (and color and line strength), resampling them on to the chosen output grid, and combining them into final library spectra.

The selected grid of spectral types follows closely the types published by Sviderskiene (1988), which combines extensive spectral energy distribution (SED) data of normal stars on a common system normalized to the energy distribution of Vega (Hayes & Latham 1975). It is extended here to include additional non-solar abundance components where such data exist.

2. DATA SOURCES

The chosen input sources are listed in Table 1, which summarizes their spectral type and luminosity class coverage, the

TABLE 1
STELLAR LIBRARY INPUT SOURCE SUMMARY

Input Source	Spectral Types	Luminosity Classes	$N_{\text{avail}}/N_{\text{used}}$	$\lambda\lambda$ Range (Å)	R	Å Pixel ⁻¹	× Bin ^a	Usage	References
SVID ^b	O–M	I–V	98/98	1200–10500	50	50	...	SED, uv for late types	1
IUE	O–G	I–V	229/173	1153–3201	500	2	2	uv for early types	2
GS	O–M	I–V	175/170	3160–10620	250	10/20	...	3200–3500 Å, 9000–10620 Å	3
KIEHL	F–M	I–V	60/59	3200–8800	500	10	...	Where available	4
JHC	O–M	I–V	161/157	3510–7427	1200	1.4	3	Where available	5
SC	O–M	I–V	72/52	3510–8930	500	5	...	Some doubtful types	6
PIC	O–M	I–V	48/34	3600–10000	500	3	2	excluded	7
N6522	K	III	16/15	3800–6800	400	6	...	3900–10000 Å Where available	8
SRBJ	GKM	I/III	21/19	4800–8920	6000	0.43	10	Where available	9
SRBJ	GKM	I/III	7/7	5000–9783	1000	3.3	2	Where available	9
DD	O–M	I–V	130/121	5804–10200	800	4	...	Contin. fitted to SVID or GS	10
LRV	O–M	I–V	84/83	14300–25000	500	~7	...	Where available	11
DBJ	O–M	I,III,V	40/36	15700–165000	2000	3/6	2/1	Where available	12
KH	F–M	I–V	26/24	20100–24100	3000	~2	4	Contin. fitted to LRV or COHEN	13
COHEN	AGKM	III,V	14/8	10000–350000	100	100	...	Where available	14
FLUKS	M	III	11/11	995–125000	5000	1	8	Synthetic MIII spectra	15

^a Binning of data prior to combination; the *IUE*, *JHC*, and higher resolution *SRBJ* data were also slightly Gauss filtered to match other data sets and conform to the chosen output resolution.

^b SVID spectra were used to define the spectral energy distribution (SED) for most types and to check other input spectra flux calibrations. They were included in the final combination when no other spectra were available; the uv of some late types, and a few other wavelength gaps.

REFERENCES.—(1) Sviderskiene 1988; (2) Heck et al. 1984; (3) Gunn & Stryker 1983; (4) Kiehling 1987; (5) Jacoby et al. 1984; (6) Silva & Cornell 1992; (7) Pickles 1985; (8) Pickles & van der Kruit 1990; (9) Serote Roos et al. 1996; (10) Danks & Dennefeld 1994; (11) Lancon & Rocca-Volmerange 1992; (12) Dallier et al. 1996; (13) Kleinmann & Hall 1986; (14) Cohen et al. 1995, 1996a, 1996b; (15) Fluks et al. 1994.

number of available spectra and those actually used, their wavelength coverage, resolution, and sampling. Based on the available libraries, the output wavelength grid was chosen to be 1150–25000 Å with a sampling interval of 5 Å pixel⁻¹ and resolution of ~500, which is the highest resolution for which full coverage is available. There are higher resolution source spectra but not enough to cover the wavelength or abundance range adequately. Higher resolution source spectra were binned and/or filtered to provide a chosen output resolution of about 500 over most of the wavelength range. This resolution is insufficient to measure adequately some fine spectral indices known to discriminate between age and metallicity in composite systems (Rose 1994; Jones & Worthey 1995) but is

adequate for resolving many other useful luminosity- and metallicity-sensitive features (Faber et al. 1985; Pickles & van der Kruit 1990) and the Balmer lines including H δ . Projects requiring higher resolution, particularly around the 4000 Å break, normally have smaller spectral coverage and can use higher resolution sources directly.

The spectral combination was done in two stages. First, the library was formed from the ultraviolet, optical, and near-infrared sources in the wavelength range 1150–10620 Å. This library has complete spectral coverage for all components (including metal-weak and metal-rich components) over this wavelength region and is referred to as UVILIB. Second, the UVILIB spectra were combined with additional infrared data

TABLE 2
STELLAR LIBRARY COMPONENTS, PHYSICAL DATA, AND SYNTHETIC PHOTOMETRY

N (1)	Components ^{a, b} (2)	Type ^c (3)	$\log T_e$ (4)	$U_3 - V$ (5)	$B_3 - V$ (6)	$V - R_c$ (7)	$V - I_c$ (8)	$V - J$ (9)	$V - H$ (10)	$V - K$ (11)	[Fe/H] ^d (12)	M_{bol} (13)	BC_V^e (14)
1	1710 310002 3000	O5 V	4.600	-1.48	-0.38	-0.17	-0.36	-0.74	-0.99	-1.10	0	-8.9	-3.7
2	1310 600001 2100	O9 V	4.550	-1.39	-0.33	-0.19	-0.35	-0.72	-0.90	-0.99	0	-7.8	-3.3
3	1210 210001 1100	B0 V	4.450	-1.33	-0.34	-0.16	-0.31	-0.70	-0.83	-0.86	0	-5.9	-2.4
4	1710 101003 0000	B1 V	4.350	-1.14	-0.24	-0.12	-0.24	-0.63	-0.73	-0.78	0	-4.7	-2.0
5	1720 400011 1200	B3 V	4.280	-0.86	-0.20	-0.10	-0.15	-0.48	-0.73	-0.80	0	-3.5	-1.5
6	2720 200011 0000	B5-7 V	4.150	-0.55	-0.14	-0.07	-0.08	-0.32	-0.37	-0.40	0	-1.0	-1.0
7	1610 000001 0000	B8 V	4.070	-0.34	-0.11	-0.03	-0.06	-0.23	-0.26	-0.28	0	-2.1	-0.6
8	1310 001001 0000	B9 V	4.030	-0.20	-0.04	-0.34	-0.04	-0.14	-0.15	-0.16	0	-1.0	-0.8
9	1420 211001 1002	A0 V	3.980	0.04	0.02	-0.01	0.01	-0.18	0.00	-0.01	0	0.3	-0.3
10	1210 300002 1000	A2 V	3.950	0.10	0.03	0.01	0.05	-0.02	-0.15	-0.14	0	1.1	-0.08
11	1520 110000 1000	A3 V	3.944	0.15	0.09	0.04	0.10	0.04	-0.13	-0.13	0	1.3	-0.03
12	1430 101001 0000	A5 V	3.929	0.24	0.15	0.05	0.16	0.29	0.35	0.36	0	1.7	0.01
13	1260 210002 0000	A7 V	3.906	0.30	0.20	0.11	0.24	0.37	0.46	0.47	0	2.1	0.01
14	1431 300010 0000	F0 V	3.858	0.35	0.30	0.18	0.38	0.53	0.66	0.68	0	3.0	0.02
15	1210 101002 2000	F2 V	3.831	0.39	0.40	0.21	0.46	0.61	0.62	0.65	0	3.3	0.03
16	1120 311000 2000	F5 V	3.815	0.42	0.46	0.24	0.50	0.83	1.03	1.06	0.0	3.5	0.00
17	1110 210000 0000	wF5 V	3.820	0.35	0.44	0.25	0.51	0.78	1.01	1.04	-0.3	3.8	-0.02
18	1122 210003 2010	F6 V	3.798	0.48	0.47	0.27	0.56	0.90	1.11	1.13	0.0	3.8	-0.03
19	1110 110000 0000	rF6 V	3.786	0.56	0.51	0.30	0.60	0.95	1.21	1.24	0.3	3.3	-0.04
20	1120 410000 3100	F8 V	3.781	0.60	0.54	0.30	0.62	1.01	1.22	1.25	0.0	4.0	-0.04
21	1120 211000 0000	wF8 V	3.788	0.53	0.52	0.29	0.59	0.96	1.26	1.29	-0.5	4.3	-0.05
22	1111 200000 0000	rF8 V	3.761	0.68	0.57	0.33	0.68	1.05	1.36	1.39	0.2	3.7	-0.06
23	1120 101001 2100	G0 V	3.764	0.69	0.57	0.32	0.67	1.02	1.28	1.30	0.0	4.2	-0.04
24	1120 110000 0000	wG0 V	3.767	0.65	0.55	0.32	0.66	0.97	1.31	1.35	-0.8	4.7	-0.05
25	1110 210000 0000	rG0 V	3.751	0.77	0.59	0.35	0.72	1.08	1.40	1.44	0.4	3.8	-0.08
26	1112 210011 2021	G2 V	3.751	0.81	0.63	0.35	0.72	1.21	1.54	1.56	-0.2	4.6	-0.10
27	1110 101001 2000	G5 V	3.747	0.95	0.69	0.36	0.74	1.19	1.45	1.51	0.0	4.7	-0.08
28	1112 120000 0000	wG5 V	3.760	0.77	0.65	0.35	0.69	1.15	1.47	1.54	-0.4	5.0	-0.07
29	1111 110000 0000	rG5 V	3.748	1.00	0.70	0.38	0.73	1.22	1.58	1.63	0.1	3.9	-0.10
30	3021 220000 2100	G8 V	3.727	1.13	0.75	0.41	0.81	1.34	1.69	1.76	0.4	5.1	-0.14
31	3020 001001 0100	K0 V	3.715	1.20	0.77	0.45	0.87	1.38	1.83	1.90	0.1	5.4	-0.18
32	3011 010020 2210	rK0 V	3.719	1.40	0.83	0.46	0.85	1.50	1.96	2.02	0.5	4.7	-0.20
33	1120 001001 0200	K2 V	3.689	1.58	0.92	0.52	0.97	1.65	2.14	2.23	0	5.9	-0.29
34	3010 010010 1100	K3 V	3.653	1.73	0.93	0.60	1.11	1.81	2.37	2.40	0	6.4	-0.40
35	3021 101000 0000	K4 V	3.638	1.95	1.09	0.66	1.23	1.97	2.54	2.64	0	6.7	-0.51
36	3010 000000 0000	K5 V	3.622	2.34	1.21	0.75	1.36	2.17	2.77	2.87	0	7.0	-0.64
37	3040 200000 2100	K7 V	3.602	2.46	1.38	0.83	1.58	2.40	2.97	3.09	0	7.4	-0.81
38	3010 000001 0000	M0 V	3.580	2.51	1.32	0.86	1.71	2.86	3.51	3.68	0	7.5	-1.12
39	4000 001011 0000	M1 V	3.566	2.58	1.38	0.88	1.87	2.97	3.62	3.90	0	7.8	-1.25
40	3020 010001 1010	M2 V	3.550	2.50	1.44	0.96	2.02	3.29	3.96	4.14	0	8.1	-1.48
41	3000 001001 0200	M2.5 V	3.537	2.67	1.50	1.02	2.25	3.56	4.20	4.41	0	8.4	-1.71
42	3010 210000 0000	M3 V	3.519	2.57	1.52	1.07	2.44	3.82	4.45	4.67	0	8.7	-1.93
43	3010 001000 0000	M4 V	3.493	3.01	1.59	1.22	2.78	4.42	5.04	5.31	0	9.1	-2.44
44	3010 001000 1010	M5 V	3.470	3.02	1.66	1.37	3.14	5.25	6.10	6.39	0	9.5	-3.22
45	3010 000000 0000	M6 V	3.431	3.05	1.82	1.65	3.69	6.36	7.03	7.41	0	10.0	-4.2
46	0220 000011 0100	B2 IV	4.300	-1.15	-0.30	-0.13	-0.24	-0.62	-0.72	-0.74	0	-4.6	-1.9
47	0420 000000 0000	B6 IV	4.100	-0.42	-0.11	-0.04	-0.09	-0.32	-0.42	-0.45	0	-2.4	-0.8
48	0430 000001 0000	A0 IV	3.988	-0.01	-0.05	-0.01	-0.00	-0.02	0.02	-0.03	0	-0.1	-0.2
49	0220 010000 0000	A4-7 IV	3.900	0.17	0.08	0.04	0.09	0.28	0.39	0.38	0	1.1	0.00
50	1330 210002 0000	F0-2 IV	3.847	0.36	0.34	0.20	0.41	0.59	0.70	0.74	0	2.0	0.03
51	1121 000002 1000	F5 IV	3.817	0.42	0.40	0.24	0.50	0.80	0.97	0.98	0	2.3	-0.01
52	3002 010002 1010	F8 IV	3.789	0.66	0.55	0.28	0.59	1.03	1.28	1.29	0	2.7	-0.03
53	3010 110010 0000	G0 IV	3.773	0.79	0.59	0.32	0.64	1.01	1.40	1.39	0	3.2	-0.04
54	3050 110001 0100	G2 IV	3.755	0.97	0.68	0.34	0.70	1.11	1.40	1.50	-0.1	3.1	-0.05
55	3021 111010 0000	G5 IV	3.748	1.13	0.75	0.39	0.77	1.21	1.51	1.60	0.1	3.1	-0.08
56	3030 001001 1000	G8 IV	3.725	1.37	0.82	0.45	0.86	1.40	1.74	1.80	-0.4	3.1	-0.15
57	3030 000001 0000	K0 IV	3.700	1.65	0.95	0.51	0.96	1.42	1.91	1.99	0.0	2.9	-0.21
58	3020 000000 0000	K1 IV	3.680	1.71	0.97	0.56	1.04	1.53	2.01	2.10	-0.3	2.8	-0.27
59	3040 000000 0000	K3 IV	3.660	2.34	1.18	0.62	1.17	1.83	2.32	2.41	0.0	2.6	-0.39

TABLE 2
(CONTINUED)

<i>N</i> (1)	Components ^{a, b} (2)	Type ^c (3)	$\log T_e$ (4)	$U_3 - V$ (5)	$B_3 - V$ (6)	$V - R_c$ (7)	$V - I_c$ (8)	$V - J$ (9)	$V - H$ (10)	$V - K$ (11)	[Fe/H] ^d (12)	M_{bol} (13)	BC _V ^e (14)
60	1200 510001 0000	O8 III	4.500	-1.40	-0.34	-0.16	-0.35	-0.82	-0.83	-0.95	0	-8.7	-3.1
61	1620 200003 0200	B1-2 III	4.300	-1.18	-0.26	-0.14	-0.24	-0.53	-0.62	-0.72	0	-5.9	-1.8
62	1310 200001 0000	B3 III	4.230	-0.85	-0.19	-0.12	-0.16	-0.52	-0.52	-0.54	0	-4.6	-1.4
63	1410 300003 0000	B5 III	4.170	-0.63	-0.15	-0.08	-0.10	-0.32	-0.42	-0.44	0	-3.5	-1.01
64	1410 300004 0000	B9 III	4.045	-0.17	-0.08	-0.03	-0.06	-0.12	-0.22	-0.23	0	-1.3	-0.39
65	1110 100001 0000	A0 III	3.981	0.04	0.04	0.00	0.01	-0.02	-0.02	-0.04	0	-0.4	-0.29
66	1100 200001 1000	A3 III	3.953	0.24	0.13	0.05	0.08	0.08	-0.05	-0.08	0	0.3	0.08
67	1110 100000 0000	A5 III	3.927	0.28	0.18	0.07	0.16	0.29	0.39	0.38	0	0.5	0.04
68	1300 110002 2000	A7 III	3.906	0.35	0.21	0.12	0.24	0.40	0.28	0.38	0	1.0	0.05
69	1211 101002 0000	F0 III	3.880	0.39	0.27	0.14	0.32	0.49	0.69	0.68	0	1.1	0.05
70	3000 100001 0000	F2 III	3.835	0.45	0.42	0.23	0.45	0.69	0.80	0.79	0	1.6	0.03
71	1101 411002 0000	F5 III	3.815	0.49	0.43	0.25	0.51	0.80	1.09	1.08	0	1.6	-0.02
72	3001 210000 1120	G0 III	3.749	0.94	0.66	0.37	0.73	1.31	1.74	1.76	-0.22	2.0	-0.13
73	3002 101011 3110	G5 III	3.713	1.45	0.89	0.45	0.87	1.54	2.01	2.05	-0.12	3.2	-0.21
74	3020 210001 0000	wG5 III	3.715	1.19	0.81	0.45	0.86	1.47	1.91	2.00	-0.26	2.8	-0.20
75	3002 200111 0000	rG5 III	3.709	1.43	0.87	0.47	0.89	1.62	2.11	2.21	0.23	3.4	-0.25
76	3010 310012 1110	G8 III	3.700	1.63	0.95	0.48	0.93	1.59	2.07	2.12	0.06	3.1	-0.24
77	3010 001111 0000	wG8 III	3.701	1.51	0.87	0.47	0.92	1.52	2.01	2.10	-0.38	2.7	-0.23
78	3020 001001 2121	K0 III	3.686	1.80	0.96	0.50	0.98	1.69	2.19	2.25	-0.08	3.1	-0.29
79	3020 000301 0000	wK0 III	3.697	1.53	0.95	0.48	0.94	1.62	2.11	2.20	-0.33	2.5	-0.26
80	3020 100001 0000	rK0 III	3.683	1.90	1.00	0.52	0.99	1.77	2.31	2.40	0.18	3.3	-0.33
81	3030 000001 2000	K1 III	3.668	1.99	1.04	0.54	1.04	1.82	2.33	2.41	0.09	1.8	-0.36
82	3030 001001 0000	wK1 III	3.683	1.84	1.02	0.52	0.99	1.77	2.32	2.41	-0.10	1.2	-0.33
83	3011 001210 0000	rK1 III	3.662	2.25	1.10	0.56	1.07	1.93	2.51	2.61	0.27	3.2	-0.43
84	3020 010001 2012	K2 III	3.649	2.14	1.11	0.59	1.13	1.97	2.62	2.67	0.05	0.9	-0.47
85	3020 000101 0000	wK2 III	3.666	2.06	1.04	0.54	1.05	1.92	2.51	2.60	-0.38	0.7	-0.42
86	3001 320011 0000	rK2 III	3.648	2.38	1.19	0.60	1.14	2.08	2.72	2.81	0.24	2.5	-0.52
87	3010 001001 1211	K3 III	3.640	2.44	1.21	0.62	1.17	2.22	2.95	3.11	-0.02	0.5	-0.63
88	3020 001100 0000	wK3 III	3.645	2.17	1.14	0.60	1.16	2.12	2.81	2.90	-0.36	-0.2	-0.57
89	3031 100320 0000	rK3 III	3.641	2.72	1.31	0.64	1.20	2.28	2.97	3.12	0.27	1.6	-0.65
90	3020 101000 1100	K4 III	3.626	2.98	1.43	0.71	1.34	2.42	3.21	3.38	0.09	-0.5	-0.79
91	3030 001000 0000	wK4 III	3.628	2.75	1.34	0.70	1.32	2.33	3.02	3.22	-0.33	-1.0	-0.73
92	3011 111200 0000	rK4 III	3.626	2.80	1.41	0.71	1.34	2.49	3.22	3.42	0.15	0.6	-0.83
93	3030 001002 3311	K5 III	3.603	3.07	1.42	0.78	1.54	2.67	3.40	3.57	-0.09	-1.3	-0.98
94	3020 011111 0000	rK5 III	3.601	3.24	1.50	0.81	1.57	2.75	3.53	3.72	0.08	-0.3	-1.05
95	1031 100000 0010	M0 III ^f	3.582	3.02	1.43	0.80	1.65	2.81	3.68	3.81	0	-1.9	-1.24
96	1001 011010 0110	M1 III ^f	3.577	3.01	1.44	0.83	1.76	2.97	3.87	3.99	0	-2.1	-1.38
97	1010 000001 1010	M2 III ^f	3.569	3.05	1.45	0.87	1.86	3.13	4.05	4.23	0	-2.3	-1.53
98	1032 110001 4100	M3 III ^f	3.560	2.95	1.43	0.91	2.08	3.44	4.36	4.54	0	-2.5	-1.81
99	1032 110010 2000	M4 III ^f	3.551	2.80	1.40	0.99	2.38	3.95	4.88	5.07	0	-2.8	-2.26
100	1031 210002 3010	M5 III ^f	3.534	2.39	1.29	1.11	2.77	4.66	5.62	5.84	0	-3.0	-2.92
101	1021 111001 0000	M6 III ^f	3.512	2.09	1.23	1.33	3.22	5.55	6.58	6.79	0	-3.5	-3.78
102	1030 000001 1020	M7 III ^f	3.495	1.43	1.09	1.65	3.81	6.76	7.82	8.05	0	-3.8	-4.95
103	1020 000001 2000	M8 III ^f	3.461	1.05	1.16	1.85	4.11	8.04	9.08	9.36	0	-4.2	-6.15
104	0000 000000 0000	M9 III ^f	3.426	0.96	1.17	1.68	3.86	8.03	8.97	9.33	0	-4.6	-6.09
105	0000 000000 0000	M10 III ^f	3.398	0.73	1.03	1.67	3.98	8.33	9.11	9.58	0	-5.0	-6.35
106	1300 100001 0000	B2 II	4.204	-1.06	-0.17	-0.12	-0.22	-0.39	-0.42	-0.43	0	-6.0	-1.2
107	1100 000001 0000	B5 II	4.100	-0.75	-0.12	-0.06	-0.15	-0.16	-0.15	-0.15	0	-5.0	-0.9
108	3001 100001 0000	F0 II	3.900	0.34	0.15	0.09	0.20	0.44	0.59	0.62	0	-2.5	0.09
109	3002 100002 0000	F2 II	3.865	0.54	0.34	0.18	0.36	0.52	0.69	0.73	0	-2.4	0.09
110	3003 200002 0000	G5 II	3.720	1.44	0.90	0.44	0.84	1.31	1.71	1.80	-0.0	-2.6	-0.12
111	4001 000011 0001	K0-1 II	3.700	2.51	1.27	0.59	1.09	1.72	2.10	2.21	-0.2	-2.8	-0.31
112	3002 000002 0001	K3-4 II	3.629	3.11	1.42	0.70	1.32	2.37	3.03	3.15	0.1	-3.1	-0.73
113	3002 000000 1000	M3 II	3.533	3.45	1.65	1.04	2.29	3.78	4.70	5.00	0	-4.1	-1.96
114	1510 200001 0000	B0 I	4.415	-1.22	-0.22	-0.13	-0.22	-0.57	-0.61	-0.71	0	-8.9	-1.8
115	1300 510000 1100	B1 I	4.316	-1.11	-0.17	-0.08	-0.16	-0.47	-0.59	-0.67	0	-8.3	-1.6
116	1100 210002 0000	B3 I	4.193	-0.90	-0.15	-0.05	-0.13	-0.30	-0.33	-0.30	0	-7.6	-1.18
117	1210 200002 0000	B5 I	4.127	-0.77	-0.06	-0.03	-0.01	-0.16	-0.15	-0.16	0	-7.2	-0.88
118	1410 100001 1000	B8 I	4.049	-0.58	-0.01	-0.03	0.03	-0.04	-0.09	-0.04	0	-6.9	-0.26

TABLE 2
(CONTINUED)

<i>N</i> (1)	Components ^{a,b} (2)	Type ^c (3)	$\log T_e$ (4)	$U_3 - V$ (5)	$B_3 - V$ (6)	$V - R_C$ (7)	$V - I_C$ (8)	$V - J$ (9)	$V - H$ (10)	$V - K$ (11)	[Fe/H] ^d (12)	M_{bol} (13)	BC_V ^e (14)
119	1100 300001 0000	A0 I	3.988	−0.24	0.00	0.02	0.07	0.10	0.19	0.16	0	−6.7	−0.18
120	1400 100001 0000	A2 I	3.958	−0.13	0.10	0.06	0.12	0.20	0.32	0.30	0	−6.7	−0.04
121	1402 400003 1000	F0 I	3.886	0.43	0.20	0.12	0.31	0.44	0.56	0.58	0	−6.6	0.10
122	1100 300001 1000	F5 I	3.822	0.47	0.27	0.18	0.39	0.66	0.76	0.77	0	−6.6	0.07
123	1101 200001 0000	F8 I	3.785	1.00	0.60	0.28	0.50	0.86	1.14	1.20	0	−6.6	0.08
124	3001 110002 0010	G0 I	3.741	1.21	0.78	0.38	0.67	1.04	1.37	1.46	0	−6.6	0.00
125	3001 300012 1100	G2 I	3.724	1.51	0.90	0.42	0.75	1.16	1.48	1.49	0	−6.5	−0.02
126	3002 100001 0000	G5 I	3.703	1.86	1.07	0.47	0.83	1.32	1.71	1.80	0.1	−6.5	−0.09
127	1101 210000 1010	G8 I	3.662	2.35	1.21	0.59	1.01	1.48	1.77	1.81	0.0	−6.5	−0.18
128	3000 110001 1000	K2 I	3.629	3.10	1.50	0.70	1.26	1.85	2.18	2.27	−0.2	−6.6	−0.40
129	3001 110021 1000	K3 I	3.616	3.23	1.57	0.78	1.39	2.18	2.74	2.83	−0.1	−6.6	−0.63
130	3002 000021 1110	K4 I	3.601	3.34	1.66	0.84	1.63	2.74	3.45	3.65	−0.2	−6.7	−1.04
131	3001 310001 2210	M2 I	3.538	3.48	1.73	1.06	2.24	3.32	3.97	4.29	0	−8.3	−1.57

^a For each library spectrum, the number of input spectra used from each of the first 14 sources listed in Table 1.

^b For input spectra from Sviderskiene 1988 listed in the first column: (1) indicates a spectrum used to check the SED, but not included in the combination; (2) indicates the average of two spectra used similarly; (3) indicates a spectrum that was actually used in the combination, generally in the uv ; and (4) indicates the average of two spectra used similarly.

^c A prefix “w” indicates metal-weak abundance; a prefix “r” indicates metal-rich abundance.

^d Abundance estimated from the Mg b /Mg H and Fe blend features.

^e $M_V = M_{\text{bol}} - \text{BC}_V$.

^f The Fluks et al. 1994 spectra are included in the M-giant library spectra only.

to a long-wavelength limit of 25000 Å to form what is referred to as the UVKLIB library. Both libraries are referred to collectively as HILIB.

3. COMPONENT COMBINATION: 1150–10620 Å

All the available digital components were initially assigned to a library component according to their spectral type, luminosity class, and chemical abundance. Stellar classifications and component groupings were checked against the SIMBAD database operated at Centre de Données Astronomiques, Strasbourg, France, and from the colors and line strengths measured from the spectra themselves.

For each library component, input spectra were read in and converted if necessary to flux per unit wavelength versus wavelength. These spectra were binned and filtered if necessary (see Table 1) to reduce them to a common resolution of about 500, which is a compromise from among the input data. The input spectra were then normalized to unity at 5556 Å and inspected for conformity with each other and with an appropriate SED; some spectra were adjusted by division by a smooth curve to remove residual flux calibration errors (see § 3.4). The input spectra were then resampled on to the chosen output grid, combined into final library spectra, and inspected again. Based on this interactive and sometimes iterative analysis, some spectra were adjusted by type slightly (one or two classes) if the measured colors warranted. Additional metal-weak and metal-rich library components were added where sufficient data existed—the GK dwarf and giant branches.

Table 2 lists the final library components by type, together with the number of spectra from each source actually used in

the combination. There are potentially nine sources in this wavelength range, although in practice the maximum number of such sources for any library spectrum was 7 (e.g., G2 V; see col. [2] of Table 2). The complete assignment of stars by source, name, and type for each library component is summarized in a data file “sources,” which is rather extended and is available electronically (see § 6).

For the actual combination, multiple spectra from each source were first averaged independently, and their standard deviation calculated. Spectra from each source were then re-sampled by cubic spline interpolation on to the output wavelength grid 1150–10620 Å and set to zero outside of their valid regions or within atmospheric windows where their definition was poor. The data combination is such that valid (nonzero) contributions from the available (preaveraged) source components became the output library spectrum in wavelength regions in which only one source exists. Where multiple sources exist, they were averaged and their standard deviation calculated for each wavelength point. Discrepant points were then discarded if necessary and the process repeated. In practice, however, discrepant data were avoided by explicitly setting to zero those parts of source spectra that deviated significantly from the appropriate standard spectral energy distribution from Sviderskiene (1988) or Gunn & Stryker (1983), and there were few pixel rejections in the formal combination.

The standard deviation curve associated with each library spectrum is that of the combination of (preaveraged) sources for wavelengths in which multiple sources exist, is the standard deviation of the average from one source when there are multiple spectra from only one source, and is zero when only one

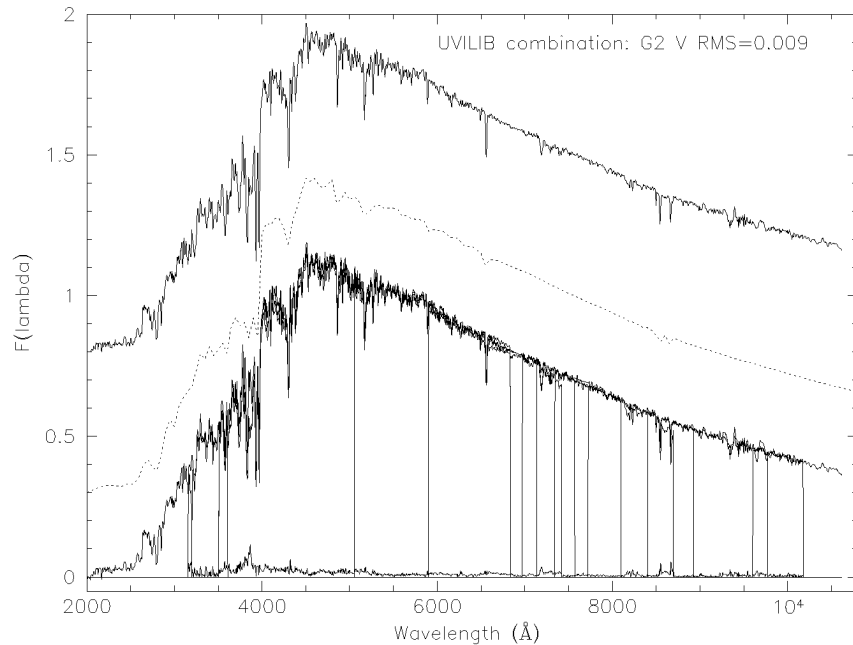


FIG. 1.—Example of the spectral combination process for the G2 V UVLIB component. As listed for component 26 in Table 2, this includes one reference SED spectrum from Sviderskiene (1988; the dotted line shown offset by 0.3 here, but not included in the combination), one *IUE* spectrum from Heck et al. (1984), one from Gunn & Stryker (1983) that is used in the blue and red, two from Kiehling (1987, with a formal rms error on their individual average of 1.1%), two from Jacoby et al. (1984; rms: 1.4%), one from Silva & Cornell (1992), one from Serote Roos et al. (1996), and one from Danks & Dennefeld (1994). Vertical lines indicate the start and end wavelength regions of the various components, together with atmospheric regions explicitly set to zero. The final combination spectrum, which is the average of all nonzero contributions, is shown offset (by 0.8) above, and the standard deviation curve from the combination is shown at bottom, with a formal rms error of 0.9% over the full wavelength range.

input spectrum defines the library spectrum. This error curve is tabulated with the library spectra for each wavelength point in the electronic distribution, as are the preaveraged spectra from each available source (see § 6).

The SM plotting and vector arithmetic package (Lupton & Monger 1997)¹ was used to read, display, filter, spline, and combine all data. The SM macros to do this are not included in the electronic distribution but are available on request from the author if combinations of additional data are desired.

3.1. Sviderskiene

This comprehensive study (Sviderskiene 1988) of the energy distribution of stellar spectra provides the basis of the stellar type component selection presented here. The library consists of 98 spectra covering a wide range of standard spectral types and all luminosity classes at solar abundance, with spectral coverage from 1200 to 10500 Å in 50 Å steps, and one additional flux point at 12500 Å. The flux library has insufficient resolution (50) for our purposes here, but its scope, consistency, and accuracy of energy distribution make it an ideal check on all other input spectra for flux calibration and accuracy. Data

from this library were used to provide ultraviolet coverage for some later spectral types lacking *IUE* data, however, as identified in the first digit of the second column of Table 2. The 98 types form the basis for each of the solar abundance components in the HILIB library. This component number has been extended here to 131 by the inclusion of additional metal-weak and metal-rich components where the available data permit: G- and K-type dwarf and giant spectra.

This library and earlier versions (Straizys & Sviderskiene 1972) are also used to generate and check synthetic photometry of digital spectra of standard stellar types.

3.2. Ultraviolet

The *IUE* atlas (Heck et al. 1984) of 229 low-dispersion spectra from the *International Ultraviolet Explorer* satellite provides ultraviolet coverage for earlier spectral types O–F, with some G-type spectra. It covers the wavelength range 1153–3201 Å in 2 Å steps at a resolution of 500. Spectra were combined by type and luminosity into the component types described above and checked against the reference SED from Sviderskiene (1988). The original spectra were double binned, averaged by type, and then Gauss filtered slightly to match better the resolution of the adjacent longer wavelength components. The individual rms errors (averaged over 1150–3200

¹ Available electronically at URL <http://www.astro.princeton.edu/~rhl/sm/sm.html>.

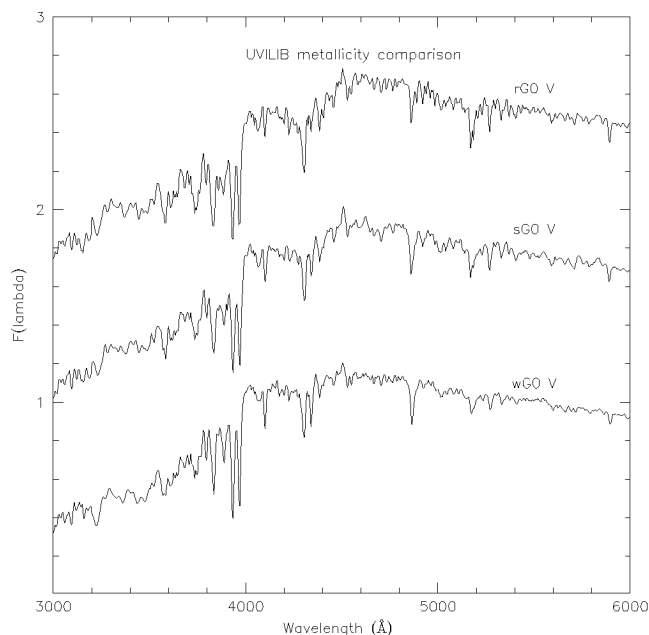


FIG. 2.—Examples of UVILIB spectra showing the metallicity range for the G0 V components. The metal-weak library spectra represent stars about one-half solar metallicity, and the metal-rich spectra represent stars about twice solar metallicity. The strengths of the Balmer lines ($H\delta$ 4101, $H\gamma$ 4340, and $H\beta$ 4861) decrease, while the strengths of the Mg H/Mg b feature at 5175 Å and Fe I blends ($\lambda\lambda$ 4385, 5270, 5330) increase going from metal weak to metal rich.

Å) of the *IUE* spectral averages by component are generally of the order 1%–2%; they are not tabulated here but are listed in the headers of the appropriate spectral data files contained in the electronic distribution (see § 6).

The earliest (O) type spectra are particularly divergent owing to variable amounts of close-in dust absorption. Only spectra that reasonably matched the chosen SED from Sviderskiene (1988) were included. The resultant O5 V, O9 V, and O8 III spectra are therefore only broadly representative of the emergent spectra from these classes.

3.3. Optical

The stellar atlas of Gunn & Stryker (1983) contains 175 dereddened and well-calibrated spectra covering all normal spectral types and luminosity classes. The spectral coverage extends from 3160 to 10620 Å, in steps of 10 Å in the blue and 20 Å in the red. The resolution of 250 is unfortunately lower than desired for full inclusion in this library, but these spectra are used to check further the SED of other components in order to bridge the gap 3200–3500 Å where necessary, and sometimes in the red from ~9000 to 10620 Å. About 20 spectral types were modified (slightly, see the data file “sources”) from the original reference to that assigned by SIMBAD. About five spectra were not used because of uncertainties in their SED or

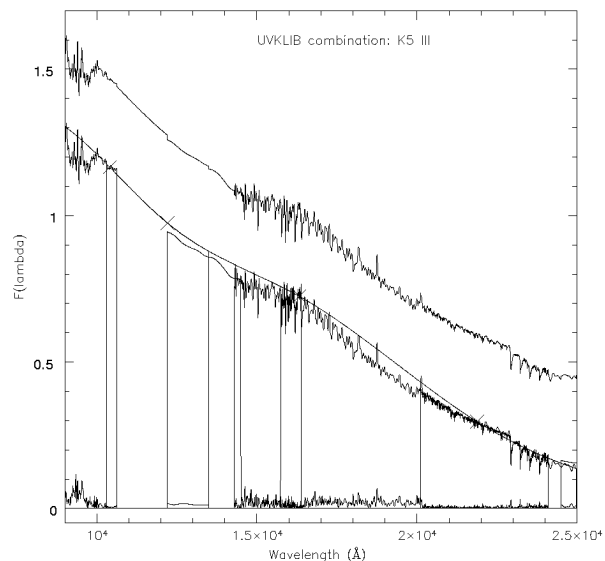


FIG. 3.—Example of the infrared spectral combination process for the K5 III UVKLIB component. This includes the preformed UVILIB K5 III spectrum, three spectra from Lancon & Rocca-Volmerange (1992, with a formal rms error on their individual average of 1.9%), three from Dallier et al. (1996; rms: 1.6%), one from Kleinmann & Hall (1986), and one from Cohen et al. (1996a), which is used here between 1.22 and 1.45 μ m and at 2.5 μ m. The crosses show the infrared flux points through which a smooth curve is fitted. This curve is included in the combination between 1.03 and 1.25 μ m. The curve at the bottom shows the standard deviation of the individual average from 1.43 to 2.02 μ m and of the combination of averages to longer wavelengths.

spectral type. Either HD 11004 is misclassified or the wrong star was observed.

The line strengths of selected features were measured for these (and all other input) spectra to group them as metal-weak, solar, or metal-rich abundance (see § 3.6 and the data file “sources”). A few spectra from this atlas were included in metal-weak and metal-rich components, but most are of solar abundance.

The atlas of Kiehling (1987) contains accurate spectrophotometry of 60 southern and equatorial stars of F–M spectral types and all luminosity classes. The wavelength coverage is from 3200 to 8800 Å in steps of 10 Å, which undersamples the original resolution. All spectra except one are used over their complete wavelength range available, but the atmospheric bands at 6800 and 7500 Å are explicitly set to zero and are therefore excluded from the final combination. About 11 spectra were classified as metal-weak or metal-rich in the combination, based on their measured line strengths (see Table 2 and the data file “sources”).

The library of Jacoby, Hunter, & Christian (1984) contains 161 relatively high resolution spectra covering all normal spectral types and luminosity classes. There is some non-solar abundance coverage, with about 22 spectra assigned to metal-weak or metal-rich components. The wavelength coverage is

from 3510 to 7427 Å in steps of 1.4 Å. The data were triple binned and averaged by type. The average spectrum was also slightly Gauss filtered prior to combination so as to match other input sources. The atmospheric bands were explicitly set to zero. About 21 spectral types were changed slightly from the original reference to that assigned by SIMBAD (see the data file “sources”).

Each spectrum in the library of Silva & Cornell (1992) is itself a compilation of several observations of stars chosen to be of similar spectral type. It contains 72 standard spectra, covering all spectral types and luminosity classes, and several metal-weak and metal-rich types. The wavelength coverage extends from 3510 to 8930 Å, but the atmospheric bands at 6800, 7200, 7500, and 8200 Å are explicitly set to zero in the original data. Some of the original spectral type and luminosity class assignments conflict with those according to SIMBAD, and these group spectra were not used. About 50 were included where appropriate, however, including 14 of non-solar abundance (see Table 2 and the data file “sources”).

The library of Pickles (1985) is another example in which each spectrum is itself a combination of observations of stars of similar types. It contains 48 standard spectra, covering all spectral types and luminosity classes, and several metal-weak and metal-rich types. The wavelength range is from 3600 to 10000 Å at 3 Å per step but is poor in the blue and is used here from 3900 to 10000 Å. The data were double binned prior to combination. Again some types are not used because of apparent mistyping of some input spectra or because they fail to match the chosen SED templates adequately. About 34 group spectra were included in the combination, including eight of non-solar abundance (see Tables 2 and the data file “sources”).

Pickles & van der Kruit (1990) presented a stellar flux library formed by combining several of the above sources. This represented an early attempt to build a comprehensive stellar library useful for modeling composite stellar systems and for generating a spectral representation of isochrone models of single stellar populations. The observations of 15 metal-weak and metal-rich giants in the nuclear bulge of our Galaxy are used here to extend the metallicity coverage (and utility) of the present library. The wavelength coverage is from 3800 to 6800 Å.

3.4. Near-Infrared

The atlas of Serote Roos, Boisson, & Joly (1996) contains high-resolution, near-infrared flux-calibrated spectra of 21 giant and supergiant stars of spectral type G–M, of which about half are super-metal rich (SMR). The wavelength coverage is 4800–8920 Å at 0.43 Å pixel⁻¹. These data were binned by 10 and slightly Gauss filtered to match the output resolution prior to combination. The atlas also contains spectra of seven dwarf and giant stars of spectral type F–M, observed at lower resolution over the wavelength range 5000–9783 Å at 3.3 Å pixel⁻¹. These data were double binned prior to combination.

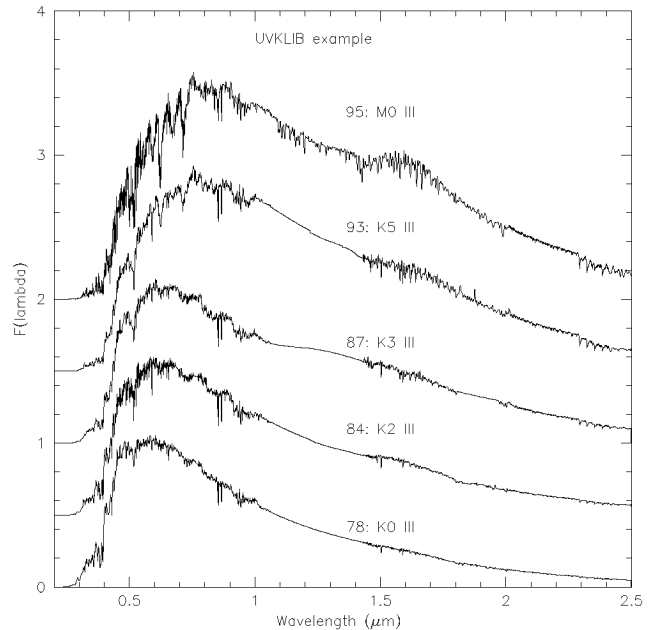


FIG. 4.—Examples of the UVKLIB library. The K giant spectra include a smooth fit between 10500 and 14300 Å, whereas the M giant spectrum includes data from Fluks et al. (1994) over this region.

The atlas of Danks & Dennefeld (1994) provides near-infrared coverage of 126 MK standards covering all normal spectral types and luminosity classes, together with a few peculiar stellar spectra. The wavelength coverage is from about 5800 to 10200 Å at 4 Å pixel⁻¹. This library provides good spectral feature definition for many library components not otherwise represented in this wavelength regime, which includes important luminosity- and metallicity-sensitive features such as the near-infrared Na I lines, Ca II triplet, TiO, and CN features. The data unfortunately suffer from rather poor flux calibration, however. A possible alternate source of digital spectra for normal stellar types in this wavelength regime is the spectrophotometry of 61 O–M stars in the wavelength range 5750–8950 Å (Torres-Dodgen & Weaver 1993). This alternate source has lower spectral resolution and again suffers from rather poor flux calibration. The atlas of Danks & Dennefeld (1994) was therefore preferred here because of its greater resolution, wavelength coverage, and number of spectra. However, each spectrum was divided by a smooth curve prior to combination to force the continuum to match the relevant spectrum from Sviderskiene (1988) or Gunn & Stryker (1983). About 30 spectral types were changed slightly from the original reference to that assigned by SIMBAD, and nine spectra were assigned to non-solar abundance components (see Tables 2 and the data file “sources”).

3.5. Accuracy of the Combination

Figure 1 shows an example of the UVLIB spectra for the G2 dwarf component and is intended to illustrate the typical

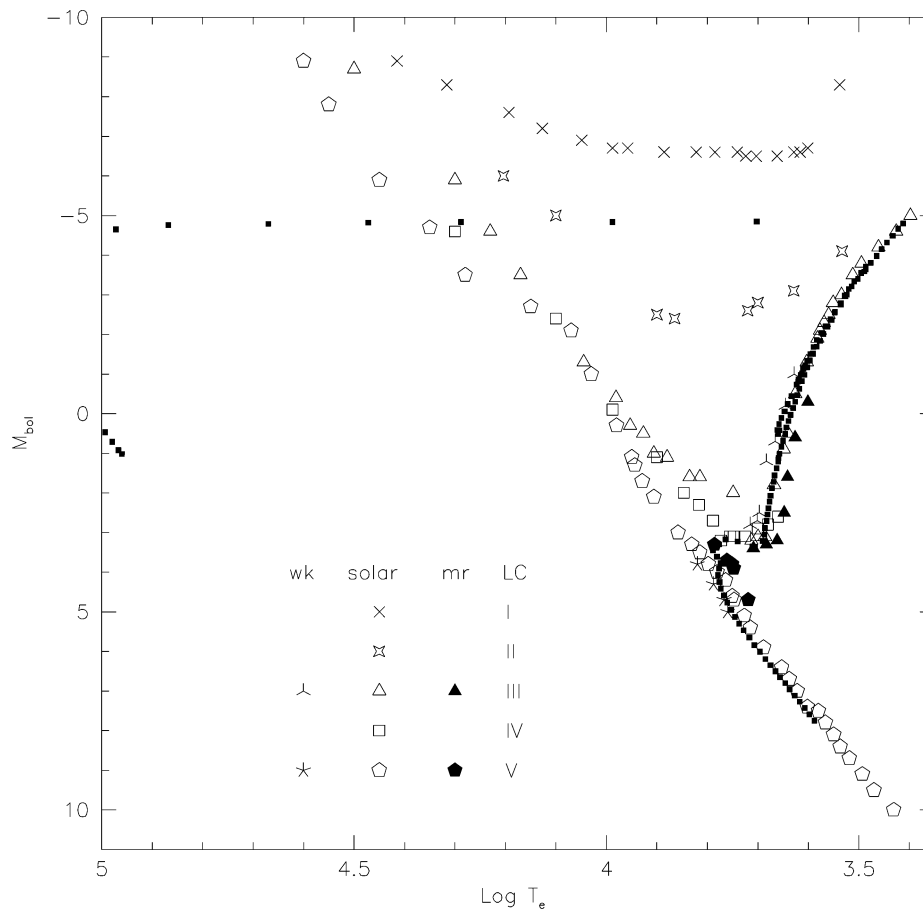


FIG. 5.—Evolutionary points (EPs: *small filled squares*) for a solar-age, solar-metallicity isochrone from Bertelli et al. (1994), plotted as bolometric magnitude vs. $\log T_e$, with the library flux points overplotted and distinguished by metallicity and luminosity class. Not all the white dwarf EPs are shown.

“best” and “worst” features of the combination. There are some regions of poor correspondence, e.g., that of strong metal and CN absorption blueward of the Ca II K and H lines and around the Ca II triplet. The first is due to real variation among the input spectra in this narrow region, despite their similarity of type, color, and other line strengths: this component therefore represents an “average” of real variation within this wavelength region for this type. The second is possibly due to poor calibration of one input spectrum. Some combinatory improvements could be made by applying more vigorous flux adjustments to more of the input spectra, but the approach adopted is to use most input spectra as published where possible. The generally very high degree of correspondence between the various overlapping components is evident. The rms errors of the individual averages from each input source are generally better than 2%. The rms errors of the combination of sources into each library component (which are listed with the library spectra available electronically) are typically 1%–2% or better, which reflects the generally high accuracy of the input observations themselves and the good correspondence achievable

between sources, provided that care is taken to combine them accurately by type.

3.6. Line Strengths

Line strengths for all the input and library spectra were measured as local equivalent widths, defined as

$$\text{LEW} = \Delta\lambda [1 - 2F_{\text{line}}/(F_{\text{cb}} + F_{\text{cr}})],$$

where F_{line} , F_{cb} , and F_{cr} are the average fluxes per unit wavelength within the line region and pseudo-“continuum” regions to the blue and red, respectively, and $\Delta\lambda$ is the width of the line region in Å. The bandpasses used and feature strengths measured are listed in Tables 3 and 4 (see § 6). Any other desired feature can be readily measured from the digital spectra.

Line strengths of the metallicity-sensitive Fe I blends at 4385, 5270, and 5330 Å and of the Mg H/Mg *b* feature at 5180 Å were measured for each input spectrum. The logarithm of the sum of these equivalent widths (in Å) was used to calculate a

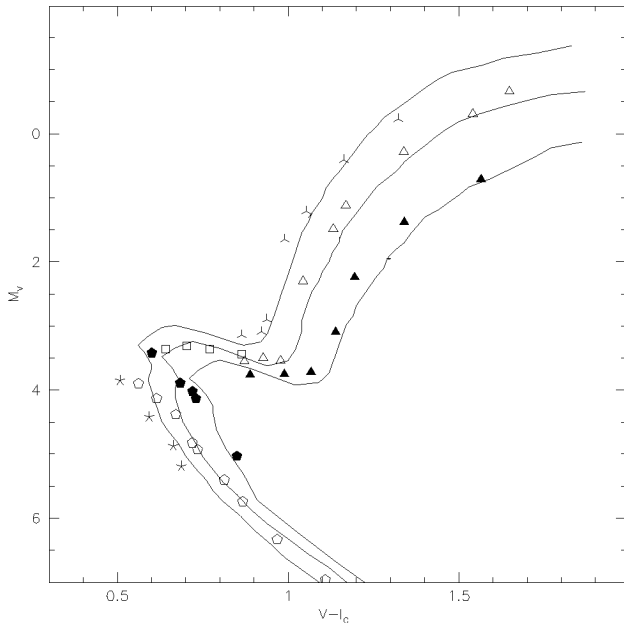


FIG. 6.—Three solar-age (5 Gyr) isochrones (lines) from Bertelli et al. (1994) of metal and helium abundance ($Z = 0.008$, $Y = 0.25$), ($Z = 0.02$, $Y = 0.28$), and ($Z = 0.05$, $Y = 0.352$) are plotted as absolute magnitude vs. $V - I_C$ color. The three isochrones illustrate the range of metallicity expected in composite populations. The G–K dwarf, subgiant, and giant library points of metal-weak, solar, and metal-rich abundance are overplotted, with the same symbol definition as in Fig. 5.

color-corrected metallicity index $[\text{Fe}/\text{H}]$ from the calibration described in Pickles & van der Kruit (1990), which follows from that first derived for K giants by Whitford & Rich (1983). This is not intended to be an accurate metallicity calibration for earlier types (or dwarfs). In fact, it underestimates metallicity for earlier types but is satisfactory for measuring relative metallicities at a given temperature and luminosity class and for sorting the input spectra into three abundance categories: “metal-weak” corresponds to abundance indicator strengths in the range 0.1–0.5 of solar; “metal-rich” corresponds to indicator strengths in the range 2–6 times solar. The estimated metallicities of the three abundance components are listed in Table 2 for the dwarf and giant branch components with sufficient source coverage to justify separate abundance classes. The es-

TABLE 3
HILIB LINE AND CONTINUUM BANDPASSES

Feature	Blue Continuum	Line	Red Continuum
G43	4260–4285	4285–4320	4320–4340
Mg <i>b</i> /Mg H	4900–4960	5160–5200	5300–5370
Mg ₂	4895–4960	5155–5200	5305–5365

NOTE.—Table 3 appears in its entirety in the electronic edition of The Publications of the Astronomical Society of the Pacific.

timated metallicities of other components are also listed, but there are insufficient data to construct components of varied metallicity in other luminosity classes.

Figure 2 shows an example of the metallicity range included among the G–K dwarfs (and giants), where the “w,” “s,” and “r” G0 V components are shown offset vertically. These three library categories correspond to approximately half-solar, solar, and twice solar abundance, although there is some abundance spread included within each component.

4. COMPONENT COMBINATION: 1150–25000 Å

There are few published digital spectral data between 1.06 and 1.43 μm . Cohen et al. (1995, 1996a, and 1996b) have published several absolutely calibrated continuous stellar spectra in the wavelength range $\sim 1\text{--}35\mu\text{m}$, of which about 14 spectra are used here. The resolution is low, but the check on spectral energy distribution is invaluable. This absolutely calibrated data was used to bridge the 1.06–1.43 μm gap where available. This is presently possible for only 12 components and, as can be seen from the last digit of the second column of Table 2, is actually used for eight components (i.e., not used for the M giant components). In these and all other cases, a smooth energy distribution was formed over the whole spectral range from ultraviolet to *L* band by splining between standard *UBVRI-JHK* flux points for each spectral type. One other flux point at 1.04 μm was included from the preformed UVILIB library. The smooth curve generated in this way was displayed and was used to check component combination and continuity in the infrared; it agrees gratifyingly well with the absolutely calibrated data when present. The smooth curve was used to bridge the wavelength gap above, to provide normalizing points for the infrared data components, and as the sole infrared component when other data did not exist.

TABLE 4
UVILIB FEATURE STRENGTH SUMMARY^a

Spectrum	Type	G43	Mg H	Mg ₂	Fe4380	Fe5270	Fe5385	H δ	H γ	H β	H α	Ca II HK	CaT	uvCN	irCN	D ₄₀₀₀	[Fe/H]
1	O5 V	0	2.1	0.05	0	0	0	2.4	1.1	3.0	2.5	1.3	0.0	0	0	0.86	0
2	O9 V	0	2.0	0.05	0	0	0.1	3.3	1.6	3.5	2.6	2.1	0.3	0	0	0.87	0
3	B0 V	0	1.9	0.05	0	0.1	0	3.3	2.4	3.5	2.7	2.4	0.5	0	1.9	0.89	0
4	B1 V	0	1.8	0.04	0	0	0.2	4.4	3.8	4.6	3.4	3.7	0.8	0.5	1.3	0.95	0
5	B3 V	0	1.6	0.04	0	0.3	0.3	6.1	6.0	6.7	5.3	4.7	2.5	1.9	0.7	1.01	0

NOTE.—Table 4 appears in its entirety in the electronic edition of The Publications of the Astronomical Society of the Pacific.

^a LEW = $\Delta\lambda[1 - 2F_{\text{line}}/(F_{\text{cb}} + F_{\text{cr}})]$. Mg₂ = $-2.5 \log (F_{\text{line}}/F_{\text{con}})$.

TABLE 5
UVI/KLIB IR STANDARD PHOTOMETRY

Spectrum	Type	$V - J$	$V - H$	$V - K$	$V - L$
1	O5 V	-0.71	-0.87	-0.91	-0.98
2	O9 V	-0.69	-0.83	-0.87	-0.93
3	B0 V	-0.67	-0.79	-0.83	-0.89
4	B1 V	-0.61	-0.71	-0.74	-0.79
5	B3 V	-0.46	-0.54	-0.56	-0.61

NOTE.—Table 5 appears in its entirety in the electronic edition of The Publications of the Astronomical Society of the Pacific.

The infrared combination consisted of reading the appropriate UVILIB data and combining them over the extended wavelength range 1150–25000 Å with available infrared components as listed in the last four digits of the second column of Table 2. When these four digits are all zero, as happens for about half of them, then the relevant UVKLIB spectrum has no observed infrared extension, and that part of the library spectrum consists solely of the smooth energy distribution matched to standard type colors. The standard color points were formed from the measured UVILIB optical data and from standard infrared color data from Bessell & Brett (1988), Koornneef (1983), and Tokunaga (1997) and from Fluks et al. (1994) for the M giants. Table 2 lists the measured synthetic colors for each library spectrum. The standard infrared component color data used to form the smooth energy curve are included as Table 5 (see § 6). Most of the metal-weak and metal-rich G–K dwarf and giant components lack infrared data; good abundance resolution is restricted to the UVILIB data. More digital spectra of non-solar abundance stars are needed, particularly at infrared wavelengths.

4.1. Infrared

The atlas of Lancon & Rocca-Volmerange (1992) provides FTS spectra of 84 stars of all spectral types and luminosity classes; the data actually used include the recalibrations from 1996. The wavelength range is large, from 1.43 to 2.5 μm at a resolution of 500. It is the existence of this extensive, well-calibrated data set that prompted and enabled this library com-

bination. The data were read as F_ν versus ν , converted to F_λ versus λ and normalized at 1.45 μm to the smooth energy distribution or data from Cohen et al. (1995, 1996a, 1996b) where available. Although generally well corrected for atmospheric absorption, some spectra are poorly defined around 1.9 μm because of strong water absorption during the observation and were set zero there prior to combination.

The atlas of Dallier, Boisson, & Joly (1996) contains medium-resolution H -band spectra of 40 stars of all spectral types and luminosity classes, including a few spectra of metal-rich stars. The wavelength range is rather narrow, from 15780 to 16420 Å at either 3 or 6 Å pixel⁻¹. The spectra were normalized at 1.6 μm to spectra from Lancon & Rocca-Volmerange (1992) and match these data rather well.

The atlas of Kleinmann & Hall (1986) contains high-resolution FTS spectra of 26 stars of spectral type F–M and of all luminosity classes. The wavelength range is from 2.01 to 2.41 μm . The data were read as F_ν versus ν , converted to F_λ versus λ , quadruple binned, and normalized at 2 μm to data from Lancon & Rocca-Volmerange (1992) or the smooth energy distribution.

Fluks et al. (1994) observed 97 M giant stars in the wavelength range 380–900 nm. The latest types are thermally pulsing, long-period variables: by observing them several times each, they were able to derive time-average spectra. Fluks et al. (1994) also constructed synthetic M giant spectra over the large wavelength interval 99–12500 nm, which are appropriate to a given average effective temperature. Each of the UVKLIB components 95–105 includes the appropriate synthetic M0–M10 giant spectra on the MK system from this work. The synthetic spectra match the spectral signatures of the observed spectra from UVILIB very well but have slightly different optical–infrared colors, with the differences increasing for later types. This may be partly because of detector linearity or dynamic range considerations for these very red stars whose red flux can be hundreds of times larger than their visual flux or because of differences between average and randomly sampled spectral signatures. The time-average spectra are considered superior for population synthesis of composite systems to other observed spectra, which sample these late-type, variable stars

TABLE 6
FILTER BANDPASSES FOR $U3$,^a $B2$,^b $B3$,^b V ,^b AND R_c ,^c AND I_c ,^c

$U3$		$B2$		$B3$		V		R_c		I_c	
λ	Trans.	λ	Trans.	λ	Trans.	λ	Trans.	λ	Trans.	λ	Trans.
3050	0.00	3600	0.00	3600	0.00	4750	0.0	5500	0.0	7000	0.0
3100	0.02	3650	0.006	3650	0.006	4800	0.03	5550	0.042	7050	0.031
3150	0.077	3700	0.023	3700	0.03	4850	0.084	5600	0.118	7100	0.074
3200	0.135	3750	0.045	3750	0.06	4900	0.163	5650	0.297	7150	0.158
3250	0.204	3800	0.106	3800	0.134	4950	0.301	5700	0.602	7200	0.314

NOTE.—Table 6 appears in its entirety in the electronic edition of The Publications of the Astronomical Society of the Pacific.

^a Buser 1978.

^b Ažusienis & Straižys 1969.

^c Bessell 1979.

TABLE 7
FILTER BANDPASSES^a FOR *J*, *H*, *K*, *L*, *L'*, AND *M*

<i>J</i>		<i>H</i>		<i>K</i>		<i>L</i>		<i>L'</i>		<i>M</i>	
λ	Trans.	λ	Trans.	λ	Trans.	λ	Trans.	λ	Trans.	λ	Trans.
10400	0.00	14400	0.00	19400	0.00	30400	0.00	34400	0.00	44400	0.00
10600	0.02	14600	0.00	19600	0.12	30800	0.02	34800	0.02	44800	0.13
10800	0.11	14800	0.15	19800	0.20	31200	0.09	35200	0.19	45200	0.34

NOTE.—Table 7 appears in its entirety in the electronic edition of The Publications of the Astronomical Society of the Pacific.

^a From Bessell & Brett 1988.

at random phases. The UVKLIB data therefore include a combination of the observed UVILIB spectra and synthetic spectra in the wavelength range 1150–10500 Å and synthetic spectra alone to longer wavelengths. These are the only components whose spectra differ in this wavelength range between UVILIB and UVKLIB.

Figure 3 shows an example of the UVKLIB spectral combination for the K5 giant component, which illustrates the good match between the various infrared components, including the smooth fit between flux points, which represent mean fluxes within the relevant filter passbands.

Figure 4 shows five examples of giant spectra from the UVKLIB library, illustrating the detail and wavelength coverage achieved, the spectral bridging between 1.05 and 1.43 μm , and the additional coverage provided for the M giants by the spectra from Fluks et al. (1994).

5. DIGITAL FILTER PHOTOMETRY

Magnitude measurements were made from the flux-calibrated digital spectra by convolving them with appropriate filter transmission profiles. In this case, the library spectra are arbitrarily normalized to unity around 5556 Å, so the magnitude measurements are relative. If T_a and ZERO_a are the transmission profile and magnitude zero point for filter “a,” then

$$\text{MAG}_a = -2.5 \log_{10} \langle F_\nu \rangle - \text{ZERO}_a,$$

where

$$\langle F_\nu \rangle = \sum (T_a F_\nu \Delta\nu) / \sum (T_a \Delta\nu)$$

and

$$\langle F_\lambda \rangle = \sum (T_a F_\lambda \Delta\lambda) / \sum (T_a \Delta\lambda).$$

Since $F_\nu d\nu = F_\lambda d\lambda$ and $d\nu = cd\lambda/\lambda^2$,

$$\langle F_\nu \rangle = \sum (T_a F_\lambda \Delta\lambda) / \sum (T_a c \Delta\lambda / \lambda^2),$$

where the last summation formula over wavelength steps is the

way $\langle F_\nu \rangle$ and hence filter magnitudes are calculated here, and

$$\langle \lambda_a \rangle = \sum (F_\lambda T_a \lambda \Delta\lambda) / \sum (F_\lambda T_a \Delta\lambda)$$

is the effective wavelength of filter “a.” Color measurements were made by differencing these filter magnitudes, and the synthetic colors were then compared to observed or standard colors for each stellar type.

5.1. Filter Transmission Profiles and Zero Points

Filter profiles for Johnson system colors *UBV* are taken from Buser (1978) for the *U3* filter and from Ažusienis & Straizys (1969) for filters *B3* and *V*. The same *V* filter profile is also used for Kron-Cousins system colors, and the R_c and I_c filter profiles are taken from Bessell (1979). The magnitude zero points for these filters were calculated by digitally photometering the standard spectra from Sviderskiene (1988) and minimizing the deviations of the measured colors from standard spectral type *UBV* colors listed in Buser (1978) and *BVRI* colors listed in Cousins (1981).

Transmission profiles for filters *JHKLL'* and *M* are from Bessell & Brett (1988). Zero points for these colors were derived simply by requiring the measured infrared colors of the A0 V library spectrum to be zero and are very close to those published in Bessell & Brett (1988).

The optical filter transmission profiles are tabulated in Table 6, and those for the infrared filters in Table 7 (see § 6). Filter zero points used here are *U3* (0.697); *B3* (−0.109); *V* (0.0); R_c (0.159); I_c (0.388); *J* (0.884); *H* (1.365); *K* (1.868); *L* (2.744); *L'* (2.941); *M* (3.389).

5.2. Library Coverage in the H-R Diagram

The synthetic colors measured from the library spectra are listed in columns (5)–(11) of Table 2. Component temperatures listed in column (4) were assigned by reference to these colors ($V - I_c$ and especially $V - K$) and Bessell (1979) and Tokunaga (1997), and to Fluks et al. (1994) for the M giant stars. The resulting $V - K$ versus $\log T_e$ calibration shows strong separation between dwarf and giant branches for M types, with M giants becoming increasingly redder with later type than dwarfs of similar effective temperature. This is noticeably different

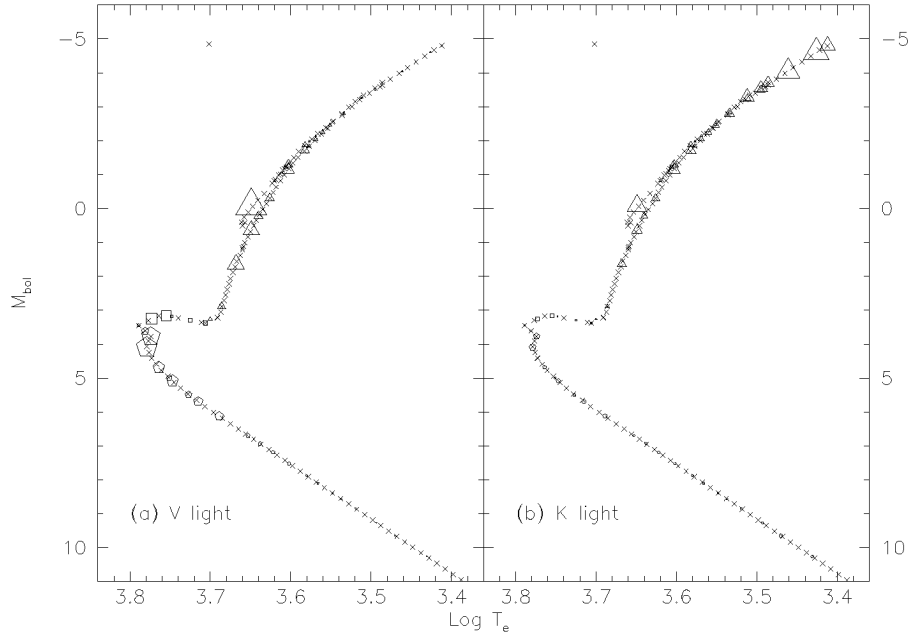


FIG. 7.—Isochrone EPs (*crosses*) extended to lower mass on the main sequence, with the library flux component points (same symbols as in Fig. 5) overplotted and sized according to (a) the *V*-light fractions and (b) the *K*-light fractions emitted by each component. Symbols at some important evolutionary phase changes represent fractional spectra interpolated between appropriate library components to accurately match the inflection in temperature (and luminosity).

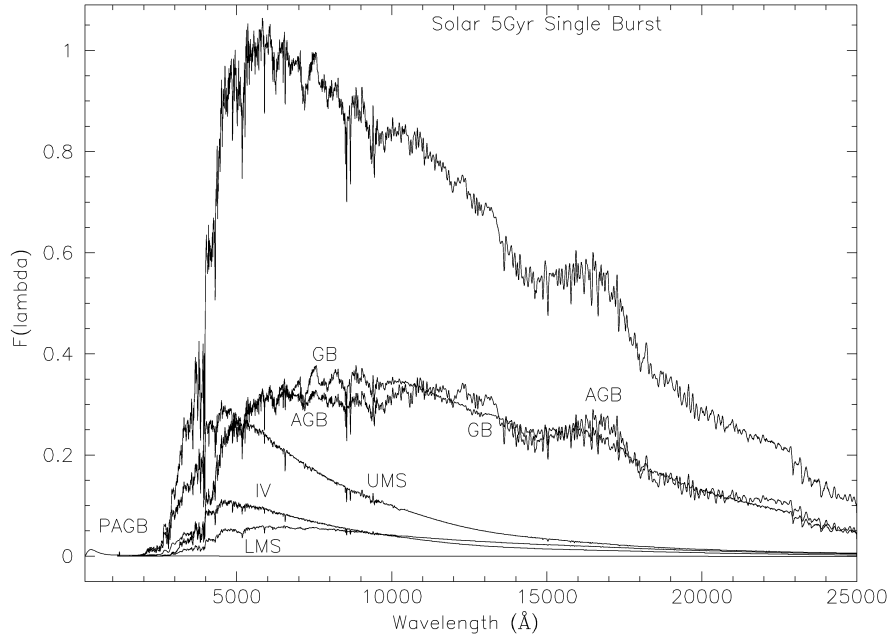


FIG. 8.—Library spectra co-added in the ratios determined from the previous figure. Spectra are grouped into lower main sequence (LMS: KM dwarfs), upper main sequence (UMS: FG dwarfs), subgiant (IV), first giant branch (GB: K–M7 giants), second and third giant branches (AGB: K–M9 III), and post-asymptotic giant branch (PAGB), which is primarily contributed by an EP at $\log T_e = 4.29$ and represented here by a combination of blackbody spectra. The top trace is the sum of the six components and represents the emergent spectrum of a single-burst stellar population of solar age and solar metallicity.

from the color-temperature relation used for late giants by Bertelli et al. (1994) for example. Their giant branch calibration bisects the dwarf and giant relationships here and is in fact closer to the dwarf relation for their latest type M giants. The effect of this difference on predicted colors of composite systems is followed in § 7.

Component bolometric corrections listed in column (14) are also assigned by reference to Bessell & Wood (1984) for most types with $V - I_c > 0$, to Lang (1992) for earlier types, and to Fluks et al. (1994, 1998), which includes absolute calibrations derived from *Hipparcos* data, for the M giant components. The temperature assignments determine the placement of components in the temperature-luminosity plane when constructing spectra appropriate to a given stellar population (see § 7). Similarly, the bolometric corrections determine the light fractions assigned to each library component in this procedure. The bolometric magnitudes listed in column (13) are of lesser importance here, since they are adjusted to match the selected isochrone values and are assigned here to match the solar-age, solar abundance isochrone from Bertelli et al. (1994).

Figure 5 shows the library points overplotted as bolometric magnitude versus $\log T_e$ on a sample solar-abundance, 5 Gyr isochrone from Bertelli et al. (1994). This figure shows the good coverage of most evolutionary stages within this plane provided by the spectral library. The library does not contain spectra to match the latest white dwarf stages of evolution, but these are minority components within this wavelength range and can be well represented by blackbody spectra.

Figure 6 illustrates the metallicity coverage available for the main-sequence turnoff, subgiant, and early giant branch regions. Solar age isochrones of approximately half-solar, solar, and twice solar abundance from Bertelli et al. (1994) are plotted as absolute magnitude versus $V - I_c$ color. The available library points of different metallicities are overlaid to illustrate the range (and the limits) of metallicity coverage afforded by the library spectra.

6. ELECTRONIC DISTRIBUTION

The electronic distribution of these data includes additional tables describing the bandpasses used for measuring line equivalent widths (Table 3) and the measured equivalent widths (Table 4), the standard component infrared color data used to form the smooth infrared energy distributions (Table 5), and the filter transmission curves used for the digital photometry (Tables 6 and 7). An extended data file ("sources") detailing the source numbers, names, and classifications of spectra used for each library component is available on request from the author.²

The UVLIB spectral library consists of 131 text files arranged in five to 10 columns, depending on the number of input components. Each file lists wavelength from 1150 to

10620 Å at 5 Å pixel⁻¹ steps in the first column, the corresponding F_λ in column (2), the standard deviation of the optical combination in column (3), and the source contributions in subsequent columns, identified by the same lettering as used in Table 2. The normalized source contributions are averages in which multiple components from a source exist. The first of three header lines summarizes rms errors of these individual averages. The standard deviation column is generally zero in wavelength regions where only one source is present, but it is sometimes replaced by the standard deviation of the average forming that single component.

The UVLIB spectral library also consists of 131 text files arranged in five to eight columns. Each file lists wavelength from 1150 to 25000 Å, at 5 Å pixel⁻¹ steps in the first column, the corresponding F_λ in column (2), the standard deviation of the combination in column (3), the spectrum from UVLIB (above) in column (4), and the infrared source spectra in subsequent columns.

7. MASPS: MAKE A STELLAR POPULATION SPECTRUM

The new library was constructed to enable detailed spectral modeling from the ultraviolet to the infrared of the emergent flux from a composite stellar system. A brief description of this application and an example are illustrated here.

An interactive C program has been written to read a selected isochrone from the extensive compilation of the Bertelli et al. (1994) co-add library spectra in the ratios appropriate to the selected isochrone and a chosen mass function and hence to derive a realistic spectral representation of the emergent spectrum from a coeval stellar population of given age, metallicity, and initial mass function. The steps involved are as follows:

1. Select and read the evolutionary points (EPs) of the chosen isochrone (age, metallicity). Each EP represents the point reached in the temperature-luminosity plane of a star of given initial mass. The isochrone tabulation lists the following for each EP: age, initial mass, temperature, bolometric and visual magnitudes, $U - B$, $B - V$, $V - R_c$, $V - I_c$, $V - J$, $V - H$, and $V - K$ colors. There are typically about 160 EPs in an isochrone tabulation from Bertelli et al. (1994).

2. Extrapolate the EPs to lower masses. Typically the isochrone tabulation extends to a lower mass of about $0.6 M_\odot$; this needs to be extended to a chosen lower mass cutoff (typically $0.15 M_\odot$) to account properly for lower main-sequence starlight. The extrapolation is linear in $\log T_e$. The latest type dwarf spectrum contained in the library is M6 V, which corresponds to stars more massive than this limit. Although the lowest mass stars contribute significantly to the mass of the composite system, they contribute very little to the emergent flux at any wavelength. Additional spectra of later type dwarfs would enhance the library's completeness but in fact would have negligible impact on the emergent flux.

3. Choose a mass function. This could be a power-law func-

² The extended data file ("sources") is also available electronically at the following URL: <http://www.ifa.hawaii.edu/~pickles/hlib.html>.

tion where a slope of $s = 2.35$ would represent a Salpeter (1955) initial mass function: this produces dwarf mass contributions (and hence M/L ratio) that increase rapidly with decreasing low-mass cutoff, although the resultant spectrum and colors are relatively insensitive to this limit within reasonable bounds. Alternatively, and as shown here, a Miller & Scalo (1979) mass function can be used: this is much less sensitive to an arbitrary low-mass cutoff and gives lower M/L ratios but in fact produces very similar spectra. The chosen initial mass function determines the number of stars at each EP and enables calculations of the total population colors from the color transformations used by Bertelli et al. (1994).

4. Select the UVKLIB spectra that most closely emulate the isochrone EPs in temperature, gravity, and abundance. In practice this means choosing dwarf and giant spectra of a given metallicity: metal-weak, metal-rich, or solar abundance; restricting the dwarf components to those appropriate to the extent of the chosen isochrone main sequence; and choosing the appropriate subgiant components and matching giant components to the first, second, and possibly third isochrone giant branch evolutionary tracks. Some important phases (e.g., at the beginning and end of evolutionary changes) are best represented by fractional UVKLIB spectra, which are interpolated in $\log T_e$ from the adjacent spectra. There are typically about 60 spectral components selected this way. Some post-asymptotic giant branch components can be represented by appropriate library components, but most (e.g., white dwarfs) require computation of blackbody spectra appropriate to the EP temperature.

5. Match the chosen spectra to (groups of) the EPs. In practice this means varying the bolometric magnitudes of the chosen spectra while maintaining their temperatures so that they slide vertically in the temperature-luminosity plane. The temperature and bolometric corrections assigned to each library spectrum are functions of their color, metallicity, and luminosity class and should remain constant as age varies. The bolometric magnitudes assigned in Table 2 are indicative values for approximately solar age and metallicity but are varied arbitrarily here to match different isochrones.

6. Interpolate the stellar numbers from the EPs to the library components, again using the chosen mass function to determine initial mass intervals between the library components. The visual light from each component can then be calculated from the bolometric magnitude appropriate to the isochrone, the assigned bolometric correction, and the relative number of stars.

7. Combine the library spectra in the ratios determined above to produce a spectrum appropriate to the chosen isochrone and mass function. The colors of the composite spectrum now depend on the library spectra colors and their effective temperature and bolometric correction assignments. These composite spectrum colors can be measured and compared with those predicted in step (3) above from the isochrone EPs and color transformation of Bertelli et al. (1994).

In principle, the transformation from the theoretical plane (luminosity and effective temperature) to the observed plane (magnitude and color), and the corresponding reverse transformation, should be symmetric. As described in § 5.2, however, these calibrations are different and need to be resolved to remove an important source of uncertainty in the modeling of composite system colors. The optical–infrared colors of the composite library spectrum derived here are redder than those predicted by Bertelli et al. (1994) because of this difference in color-temperature calibration. Work in progress should help to resolve this difference (see, e.g., Fluks et al. 1998).

Figure 7 shows the solar-age, solar abundance isochrone with the library component flux points overplotted at their fixed temperatures and adjusted bolometric magnitudes, and sized according to (a) the V -light fractions and (b) the K -light fractions emitted by each component. This diagram illustrates schematically the relative contributions of different stellar components, and can be displayed for any wavelength.

Figure 8 shows the composite spectrum obtained by co-adding the library components in the ratios determined by this procedure. The lower traces show how the partial contributions of significant evolutionary phases vary in importance with wavelength, and the upper trace shows the emergent spectrum appropriate to the (assumed single-burst) stellar population. This diagram illustrates the coverage and detail of the spectral representation which can be obtained with the new library.

8. SUMMARY

Available published spectra have been combined to provide a new library of digital stellar spectra that combines reasonable resolution with wide wavelength coverage in the range 1150–25000 Å. The library covers all normal spectral types and luminosity classes and provides some abundance resolution among G–K dwarfs and giants and is amenable to future extension. More spectra are desirable, particularly of non-solar abundance stars in the infrared. The spectra and associated tabular data are available by remote electronic access.

The library has been constructed to enable synthesis and modeling of the integrated light from composite populations. The library spectra can be combined in proportions determined by the kind of detailed isochrone tabulations of stellar systems now available (see, e.g., Bertelli et al. 1994) to produce a spectral (color and line strength) representation of any composite stellar system. There are differences, which should soon be resolved, in the color-temperature relations, with the library M giant spectra being redder in $V - K$ for a given effective temperature than tabulated in Bertelli et al. (1994).

Composite spectra of similar detail to the example shown can be constructed for any age and some abundances. Such spectra can be used to measure the detailed variation of spectral signature, color, and line strength with metallicity and age of star formation and to synthesize observed spectra and associated photometry of galaxies. The detailed variation of spectral

signature as a function of age and metallicity will be the subject of another paper.

We are grateful to the observers and authors of the data that

are combined here, to the staff of the Astronomical Data Center (Goddard Space Flight Center), and to the staff of SIMBAD and the Centre de Données Astronomiques de Strasbourg for enabling access to it and the on-line databases used here.

REFERENCES

- Ažusienis, A., & Straizys, V. 1969, *Soviet Astron.*, 13, 316
 Bertelli, G., Bressan, A., Chiosi, C., Fagotto, F., & Nasi, E. 1994, *A&AS*, 106, 275
 Bessell, M. S. 1979, *PASP*, 91, 589
 Bessell, M. S., & Brett, J. M. 1988, *PASP*, 100, 1134
 Bessell, M. S., & Wood, P. R. 1984, *PASP*, 96, 247
 Buser, R. 1978, *A&A*, 62, 411
 Charlot, S., Worthey, G., & Bressan, A. 1996, *ApJ*, 457, 625
 Cohen, M., Witteborn, F. C., Bregman, J. D., Wooden, D. H., Salama, A., & Metcalfe, L. 1996a, *AJ*, 112, 241
 Cohen, M., Witteborn, F. C., Carbon, D. F., Davies, J. K., Wooden, D. H., & Bregman, J. D. 1996b, *AJ*, 112, 2274
 Cohen, M., Witteborn, F. C., Walker, R. G., Bregman, J. D., & Wooden, D. H. 1995, *AJ*, 110, 275
 Cousins, A. W. J. 1981, *SAAO Circ.* 6, 4
 Dallier, R., Boisson, C., & Joly, M. 1996, *A&A*, 116, 239
 Danks, A. C., & Dennefeld, M. 1994, *PASP*, 106, 382
 Faber, S. M., Friel, E. D., Burstein, D., & Gaskell, C. M. 1985, *ApJS*, 57, 711
 Fluks, M. A., Plez, B., Thé, P. S., de Winter, D., Westerlund, B. E., & Steenman, H. C. 1994, *A&AS*, 105, 311
 ———. 1998, in preparation
 Gunn, J. E., & Stryker, L. L. 1983, *ApJS*, 52, 121
 Hayes, D. S., & Latham, D. W. 1975, *ApJ*, 197, 593
 Heck, A., Egret, D., Jaschek, M., & Jaschek, C. 1984, *A&AS*, 57, 213
 Jacoby, G. H., Hunter, D. A., & Christian, C. A. 1984, *ApJS*, 56, 257
 Jones, L. A., & Worthey, G. 1995, *ApJ*, 446, L31
 Kiehling, R. 1987, *A&A*, 69, 465
 Kleinmann, S. G., & Hall, D. N. B. 1986, *ApJS*, 62, 501
 Koornneef, J. 1983, *A&A*, 128, 84
 Lancon, A., & Rocca-Volmerange, B. 1992, *A&A*, 96, 593
 Lang, K. R. 1992, *Astrophysical Data* (New York: Springer)
 Leitherer, C., et al. 1996, *PASP*, 108, 996
 Lupton, R. H., & Monger, P. 1997, *The SM Reference Manual*
 Miller, G., & Scalo, J. 1979, *ApJS*, 41, 513
 Pickles, A. J. 1985, *ApJS*, 59, 33
 Pickles, A. J., & van der Kruit, P. C. 1990, *A&A*, 84, 421
 Rose, J. A. 1994, *AJ*, 107, 206
 Salpeter, E. E. 1955, *ApJ*, 121, 161
 Serote Roos, M., Boisson, C., & Joly, M. 1996, *A&A*, 117, 93
 Silva, D. R., & Cornell, M. E. 1992, *ApJS*, 81, 865
 Straizys, V., & Sviderskiene, S. 1972, *Bull. Vilna Astron. Obs.*, 35, 23
 Sviderskiene, Z. 1988, *Bull. Vilna Astron. Obs.*, 80, 1
 Tokunaga, A. T. 1997, in *Astrophysical Quantities*, ed. A. Cox (rev. 4th ed.), in press
 Torres-Dodgen, A. V., & Weaver, W. B. 1993, *PASP*, 105, 693
 Whitford, A. E., & Rich, R. M. 1983, *ApJ*, 274, 723